analytical chemistry

Article

A novel terbium functionalized micelle nanoprobe for ratiometric fluorescence detection of anthrax spore biomarker

Ke Luan, Ruiqian Meng, Changfu Shan, Jing Cao, Jianguo Jia, Wei-Sheng Liu, and Yu Tang

Anal. Chem., **Just Accepted Manuscript** • DOI: 10.1021/acs.analchem.8b00050 • Publication Date (Web): 01 Feb 2018

A novel terbium functionalized micelle nanoprobe for ratiometric fluorescence detection of anthrax spore biomarker

*Ke Luan, Ruiqian Meng, Changfu Shan, Jing Cao, Jianguo Jia, Weisheng Liu and Yu Tang**

State Key Laboratory of Applied Organic Chemistry, Key Laboratory of Nonferrous Metal Chemistry and Resources Utilization of Gansu Province, College of Chemistry and Chemical Engineering, Lanzhou University, Lanzhou 730000, P. R. China

*E-mail: tangyu@lzu.edu.cn. Fax: +86 931-891-2582.

ABSTRACT: Rapid, sensitive and selective quantitative detection of pyridine dicarboxylic acid (DPA) as biomarker of anthrax spores is in great demand since anthrax spores are lethal to human beings and animals highly and also the potential biological warfare agents. Herein, we prepared a ratiometric fluorescence lanthanide functionalized micelle nanoprobe by "one-pot" self-assembly, with an amphiphilic ligand containing β-diketone derivative which can "immobilize" terbium ions through the coordination interaction and a fluorophore as fluorescence reference (FR). The detection strategy was ascribed to Tb^{3+} ions in lanthanide functionalized micelle, which can be sensitized to emit the intrinsic luminescence upon addition of DPA due to the presence of energy transfer when DPA chromophore coordinated with Tb^{3+} ion. And the fluorescence intensity of FR remained essentially constant, leading to ratiometric fluorescence response toward DPA. The results demonstrate that the terbium functionalized micelle was able to sensitively detect DPA with a linear relation in the range of 0 μM to 7.0 μM in aqueous solution, which also showed remarkable selectivity to DPA over other aromatic ligands. Our work paves a new way in the design of ratiometric fluorescence lanthanide functionalized micelle nanoprobes which can be promising for selective and sensitive detection of bacterial spores or biomolecules.

INTRODUCTION

Bacillus anthrax, a rod-shaped, Gram-positive, and spore-forming bacterium, which can cause anthrax, further resulting in deadly infection against living organism.[1] During dormant period, the bacterial spores can survive under harsh environment such as high temperature, freeze, ultraviolet radiation, desiccation, strong acid and strong base.[2] Bacillus anthrax spores can transform into an active form when the surrounding environmental conditions are favorable. The inhalation of 10^4 B. anthrax spores is deadly, unless effective treatment is received within 24 ~ 48 h.[3-5] Accordingly the Bacillus anthrax spore as the potential biological warfare agent has attracted considerable attention around the world.[6,7] The rapid and sensitive detection of Bacillus anthrax is crucial to minimize the probability of anthrax infection and prevent bioterrorism. During the past decades, a number of sensitive, accurate and selective detection methods including biological methods, high-pressure liquid chromatography, electrochemical detection and optical methods have been developed for detecting anthrax spores.[8,9] Thereinto, optical methods such as polymerase chain reaction (PCR),[3] surface enhanced Raman spectroscopy (SERS), immunoassays and luminescence techniques for detecting anthrax spores have attracted plenty of interest.[10-13] The method of PCR assay is to amplify the bacterial DNA by chain polymerization. But it requires expensive reagents, complicated pretreatment and long test time.[3] The luminescence methods are primary based on detecting dipicolinic acid (DPA), which accounts for about 5-15% of the dry

weight of anthrax spores and is always used as a biomarker for anthrax spores.[14,15] Compared to other assays, the advantages of luminescence method show a low detection limit (LOD) for rapid, sensitive and selective response to anthrax spores.

The luminescence of lanthanide ions own intrinsic narrow f-f emission bands, long lifetimes and large Stokes shifts, which can keep off the interference from emission overlap.[16] However, f-f transition of single lanthanide ions is the Laporte forbidden, so it is significant to introduce a chromophore called "antenna" which can sensitize the lanthanide ions through the coordination interaction and energy transfer to the lanthanide ions.[17,18] Interestingly, DPA as the chromophore molecule can coordinate with lanthanide ions and achieve transfer energy to lanthanide ions, thus the sensitized lanthanide ions can exhibit characteristic luminescence emission through antenna effect.[19-21] On account of the particular intrinsic characteristics of lanthanide ions, different platforms containing lanthanide ions have been developed for anthrax spore biomarker detection such as carbon materials,[9,22-24] silica nanoparticles,[15] metal-organic frameworks,[25] and solid films.[26] To our knowledge, most of lanthanide-based sensors used to determine the concentration of DPA are according to the single change of lanthanide characteristic fluorescence intensity, and show limit of detections (LODs) varying from subnaomolar to a few tens of nanomolar of DPA.[15,27-30] However, the fluorescence intensity based on lanthanide ions always suffers from the disturbances of instrumental factors or microenvironments. To overcome these drawbacks, ratiometric fluorescence probes are

highly attractive because they are endowed with a self-calibration ability, which can reduce the aforesaid interferences.[31-33]

Self-assembled supramolecular materials derived from amphiphilic small molecule monomers have drawn more and more attention for their remarkable salient features.[34-37] The amphiphilic monomers are composed of hydrophilic part and hydrophobic part. By adjusting the structural parameters of organic structural unit, various topologies such as micelles, liposomes, and vesicles can be fabricated in aqueous solution by supramolecular self-assembly.[38,39] Recently, the self-assembly of metallo-amphiphiles has received considerable attention. These assemblies have the characteristics of organic self-assembled supermolecules, which show more sensitive to external stimuli, good biocompatibility and low cytotoxicity compared with small organic molecules. Moreover, they also display different features including in the luminescence,[40] magnetism,[41] and catalytic properties.[42] Some fluorescence nanoprobes based on self-assembly of metallo-amphipathic molecules have also been developed for detecting biomolecules.[43-44-46]

Herein, we have manufactured a ratiometric fluorescence lanthanide functionalized micelle nanoprobe that was made up of the fluorescence interior-reference and amphiphilic Tb^{3+} complexes as a “turn on” fluorescence probe by “one-pot” method in aqueous solution for the selective and sensitive detection of DPA (Scheme 1). The lanthanide functionalized micelle was constructed on the account of following

considerations: (1) Amphipathic ligand L was composed of alkyl chain moiety as hydrophobic part and hyamine moiety as hydrophilic part, which contained β-diketone derivative to "immobilize" lanthanide ions in the micelle through the coordination between the β-diketone and lanthanide ions. (2) Tb^{3+} ion was selected to coordinate with the ligand L for its characteristic emission properties, such as large Stokes shift, resistance to photobleaching, narrow emission bands and long luminescence lifetime. Its intrinsic luminescence was weak when the micelle was dispersed in aqueous solution as a result of the Laporte forbidden f-f transitions and the non-radiative transition of Tb^{3+} ion excited states to the vibrational relaxation of water molecules. Only when the lowest triplet energy level of the chromophore molecule is appropriate to the lowest triplet energy level of Tb^{3+} ions, Tb^{3+} ions can be sensitized and excited to emit intrinsic fluorescence. (3) A fluorophore as fluorescence reference (FR) which emits blue fluorescence (440 nm) at 275 nm excitation was added into the micelle. Through the above design thought, the ratiometric fluorescence terbium functionalized micelle was prepared by "one-pot" method in aqueous solution. The terbium functionalized micelle rapidly exhibited characteristic fluorescence of Tb^{3+} ions when adding DPA into the micelle solution, while the fluorescence of FR had negligible change. As far as we know, it is for the first time to achieve the detection of the anthrax spore biomarker DPA by ratiometric fluorescence terbium functionalized micelle as nanoprobe. And this design strategy can also be applied to other lanthanide micelle nanoprobes used for the detection of the biomarkers or biomolecules with high selectivity and sensitivity.

Scheme 1. Self-assembly of terbium functionalized micelle in H_2O and the response property for DPA.

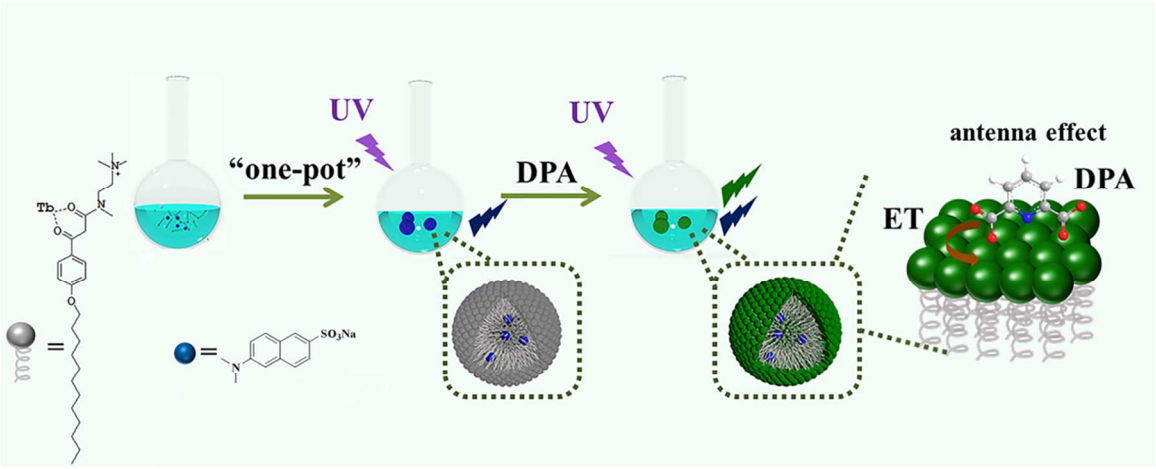

EXPERIMENTAL

Instruments and Reagent

The steady-state corrected luminescence spectra in water solution were performed on an Edinburgh Instruments FSL920 fluorescence spectrometer, with a 450 W Xe arc lamp as the steady-state excitation source. The NMR spectra were obtained on 400 MHz spectrometer with TMS as inner standard (Bruker). The UV-vis absorbance spectrum was determined on a Cary 5000 spectrophotometer (Agilent). Fourier transform infrared (FTIR) spectroscopy was obtained using FT-IR spectrometer ranging from 400 cm^{-1} to 4000 cm^{-1} by potassium bromide pellet on Vertex 70 (Burker). The surface tension (γ) was determined on Surface Tension Meter (DCAT21, Dataphysics Company, Germany) by Du Noüy ring. The morphologies of micelle were obtained on transmission electron

microscopy (Tecanai^{TM} G2 F30; FEI Company, USA) working at 300 kV. The ζ potential and the dynamic light scattering (DLS) of micelles were measured on a Zetasizer (Nano ZS, Malvern, Worcestershire, UK). Thermogravimetric analyses (TGA) were measured using a Netzsch STA 449 F3 Jupiter up to 800 °C at a heating rate of 10 °C·min^{-1} under a nitrogen atmosphere. All materials and reagents were of analytical grade and were purchased from J＆K Chemical Ltd. These reagents were used without any purification.

Synthesis of the Ligand L

The synthetic procedure of the amphiphilic ligand L is shown in Scheme 2. And the detailed synthetic route and the characterization data of the products are listed as below.

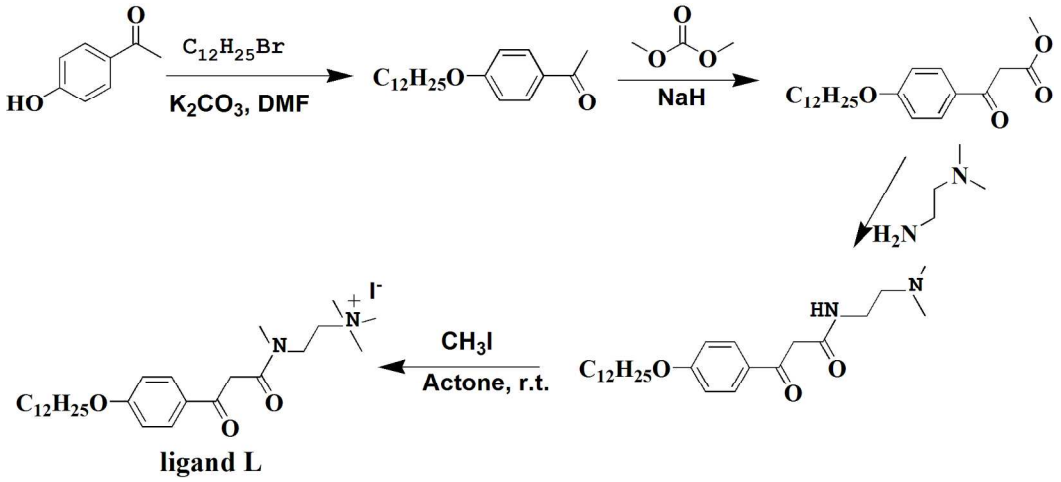

Scheme 2. Synthetic procedure of the amphiphilic ligand L.

Synthesis of 1-(4-dodecyloxy-phenyl)-ethanone: 4-Hydroxyacetophenone (4.08 g, 30 mmol) and potassium carbonate (24.8 g, 180 mmol) were dissolved in dimethyl formamide (90 mL) at room temperature, the resulting mixture was heated to 60 °C and

stirred for 1 h. Then 1-bromooctane (8.7 mL, 36 mmol) was added dropwise to the solution and stirred for an additional 12 h at 80 °C under N_2 atmosphere. After cooling, 200 mL of icy water was added to the reaction solution and the mixture was subjected to extraction with ethyl acetate (3×50 mL), collected organic layers, washed with brine (100 mL), dried over anhydrous $MgSO_4$ and concentrated under reduced pressure to give a faint yellow solid (8.1g). ^{1}H NMR (400 MHz, $CDCl_3$, ppm): δ 7.90 (d, J = 4.0 Hz, 2 H), 6.90 (d, J = 4.0 Hz, 2 H), 2.52 (s, 3 H), 1.75 - 1.70 (m, 2 H), 1.40 - 1.24 (m, 18 H), 0.86 (t, J = 7.2 Hz, 3 H). ^{13}C NMR (400 MHz, $CDCl_3$, ppm): δ 14.19, 22.77, 26.04, 26.36, 29.17, 29.43, 29.64, 29.72, 31.98, 68.30, 114.16, 130.10, 130.62, 163.18, 196.78. ESI MS (*m*/*z*): 305.3 $[M + H]^+$.

Synthesis of 3-(4-dodecyloxy-phenyl)-3-oxo-propionic acid methyl ester: Sodium hydride (0.36 g, 15 mmol) and dimethyl carbonate (0.9 g, 10 mmol) were dissolved in anhydrous methylbenzene (30 mL) and heated to 110 °C. Then 1-(4-dodecyloxy-phenyl)-ethanone (1.82 g, 6 mmol) was added dropwise to the reaction mixture over half an hour and stirred at 110 °C for 2 h. When the reaction cooled to room temperature, glacial acetic acid (1.5 mL) was slowly added and a heavy, pasty solid appeared. Subsequently icy water was added until the solid was dissolved completely. The mixture was extracted with ethyl acetate (3 × 20 mL), organic layers were combined and washed with brine, dried over anhydrous $MgSO_4$, concentrated under reduced pressure and the residue purified by column chromatography over silica gel with

petroleum ether / ethyl acetate = 10 / 1 as the eluents to give a yellow solid (1.28 g). ^{1}H NMR (400 MHz, $CDCl_3$, ppm): δ 7.90 (d, J = 8.2 Hz, 2 H), 6.92 (d, J = 8.2 Hz, 2 H), 4.02 (t, J = 6.4 Hz, 2 H), 3.94 (s, 2 H), 3.73 (s, 2 H), 1.73 - 1.68 (m, 2 H), 1.40 - 1.24 (m, 18 H), 0.87 (t, J = 7.2 Hz, 3 H). ^{13}C NMR (400 MHz, $CDCl_3$, ppm): δ 14.22, 22.78, 26.04, 29.14, 29.44, 29.63, 29.67, 29.72, 29.75, 32.00, 45.62, 52.55, 68.45, 114.47, 128.83, 131.00, 163.79, 168.32, 190.90. ESI MS (m/z): 363.30 $[M + H]^+$.

Synthesis of N-(2-amino-ethyl)-3-(4-dodecyloxy-phenyl)-3-oxo-propionamide: 3-(4-Dodecyloxy-phenyl)-3-oxo-propionic acid methyl ester (1.81 g, 5 mmol), ethane diamine (0.48 g, 8mmol), and DMAP (0.2 g, 1.5 mmol) were dissolved in 10 mL of ethanol, and then the reaction solution was stirred overnight at 78 °C. The N-(2-amino-ethyl)-3-(4-dodecyloxy-phenyl)-3-oxo-propionamide was consumed as indicated by TLC. The resulting mixture was concentrated under reduced pressure and the residue purified by column chromatography over silica gel with dichloromethane / methanol = 50 / 1 as the eluents to give a reddish brown oil (1.07 g). ^{1}H NMR (400 MHz, $CDCl_3$, ppm): δ 7.32 (d, J = 8.8Hz, 2 H), 6.86 (d, J =8.8Hz, 2 H), 3.94 (t, J = 6.4Hz, 2 H), 3.65 (s, 2 H), 3.15 (t, J = 6.4Hz, 2 H), 2.36 (t, J = 6.4Hz, 2 H), 2.17 (s, 6H), 1.79 - 1.72 (m, 2 H), 1.40 - 1.24 (m, 18 H), 0.86 (t, J = 7.2Hz, 3 H). ^{13}C NMR (400 MHz, $CDCl_3$, ppm): δ 14.16, 22.73, 26.11, 29.11, 29.27, 29.40, 29.70, 31.97, 42.68, 45.49, 50.15, 59.68, 68.06, 114.25, 128.39, 129.20, 164.66, 170.64, 190.76. ESI MS (m/z): 419.31 $[M + H]^+$.

Synthesis of the ligand L: To a solution of

N-(2-amino-ethyl)-3-(4-dodecyloxy-phenyl)-3-oxo-propionamide (0.418 g, 1 mmol) in acetone (4 mL), iodomethane (0.282 g, 5 mmol) in acetone (2 mL) was added dropwise to the solution at 0 °C. Then the reaction solution was stirred for two days at room temperature. When reaction completion, the ethyl ether (25 mL) was added, and the resulting precipitate was collected by filtration, washed with ethyl ether several times, and dried under reduced pressure to give a faint yellow solid (0.28 g). ^{1}H NMR (400 MHz, DMSO-d_6, ppm): δ 7.32 (d, J =8.8Hz, 2H), 6.97 (d, J =8.8Hz, 2H), 3.97 (t, 6.4Hz, 2H), 3.55 (s, 2H), 3.46 (t, J = 6.4Hz, 2H), 3.37 (t, J = 6.4Hz, 2H), 3.15 (s, 3H), 2.98 (s, 9H), 1.72 - 1.64 (m, 2H), 1.40 - 1.24 (m, 18H), 0.82 (t, J = 7.2Hz, 3H). ^{13}C NMR (400 MHz, $CDCl_3$, ppm): δ 14.35, 22.56, 26.10, 29.17, 29.26, 29.48, 31.78, 38.63, 50.45, 53.32, 65.10, 68.30, 86.71, 115.23, 127.45, 129.76, 160.35, 163.96, 169.80, 193.75. ESI MS (m/z): 447.44 $[M + H]^+$.

Preparation of terbium functionalized micelle

A solution of terbium(III) nitrate hexahydrate (45 mg, 0.1 mmol) in deionized water (3 mL) was added dropwise to a solution of the ligand L (57.3 mg, 0.1 mmol) in deionized water (5 mL). Then, 150 μL of sodium 6-(dimethylamino)naphthalene-2-sulfonate (FR, 10 mM, dissolved in acetone) was added to the mixture and stirred for 24 h at room temperature. Then the reaction mixture was dialyzed with a cellulose ester dialysis membrane (500 MWCO) for 2 days to completely remove "free" Tb^{3+} ions, ligand L and FR. The resulting material was dried by lyophilization to obtain micelle powder, which

was dispersed in HEPES buffer solution (10 mM, pH = 7.0) to prepare 1 mg·mL^{-1} stock solution of micelles for further characterization and use.

RESULTS and DISCUSSION

Synthesis, morphology and characterization of the terbium functionalized micelle

The sensitive and selective nanoprobe for DPA detection was based on a ratiometric lanthanide functionalized micelle, which was constructed with ligand L, Tb^{3+} ions and FR by "one-pot" method as shown in Scheme 1. The ligand L showed aggregation properties in aqueous solution due to its peculiar structure: a hydrophilic hyamine and a hydrophobic dodecyl chain. In order to investigate the self-assembly properties of micelle, critical micellar concentration (CMC) of micelle was determined by measuring the surface tension (γ) in HEPES buffer solution (10 mM, pH = 7.0) with different concentrations of Tb^{3+}-L.[47,48] With increasing concentration of Tb^{3+}-L in aqueous solution, the surface tension rapidly decline and remained steadily, which implied that the hydrophobicity of the dodecyl chain in the ligand L is enough to form micelles. The CMC was determined to be 36.4 μM from the two linear segments in the curve of γ versus concentration of the micelle solution (Figure 1a). And the successfully prepared terbium functionalized micelle was studied by transmission electron microscopy (TEM) and dynamic light scattering (DLS) in aqueous solution. The morphology of micelle was homogeneous spherical nanoparticles with an average diameter of 135 nm (Figure 1c, d),

which are features of micelles. When FR was added into the terbium functionalized micelle to construct a ratiometric fluorescence lanthanide functionalized nanoprobe, the DLS experiment showed the average diameter increased from 269.5 nm (Tb^{3+}-L micelle, without loading FR) to 271.4 nm (terbium functionalized micelle, with loading FR) (Figure S1b and Figure 1b), indicated that the load of FR had negligible effect on the particle size of terbium functionalized micelle. And the average diameter of terbium functionalized micelle determined by DLS was larger than that measured through TEM resulting from the swelling of micelles in aqueous solution.[49,50]

The coordination interaction between Tb^{3+} and the ligand L was studied by UV-vis absorption spectroscopy and Fourier Transform Infrared (FTIR) spectroscopy (Figure S2). The UV-vis absorption spectrum of ligand L showed absorption peak at 283 nm, which can be attributed to the π-π^* transition of β-diketone group.[51] In contrast, the absorption peak of Tb^{3+}-L was stronger and slightly red-shifted than the absorption peak of L, indicated that Tb^{3+} ions coordinated with ligand L (Figure S2a). When β-diketone group in the ligand L coordinates with Tb^{3+} ion, the degree of electronic delocalization is increased, and the degree of conjugation enhances, resulting in a larger activity range of π electron in the lanthanide complex. Thus, the energy for energy level transition of the associated conjugated molecular orbital is reduced, leading to the red-shifting of the absorption peak of the lanthanide complex.[52] FTIR spectrum of ligand L showed the $\nu(CH_2)$ bands at 2922 cm^{-1} and 2850 cm^{-1}, indicated the presence of hydrophobic dodecyl

chain. Besides, the sharp absorb band at 1645 cm^{-1} and 1611 cm^{-1} was ascribed to stretching vibration of carbonyl. The covalent conjugation can be confirmed by a slightly blue shift of FTIR absorption band of Tb^{3+}-L compared to the ligand L (Figure S2b).

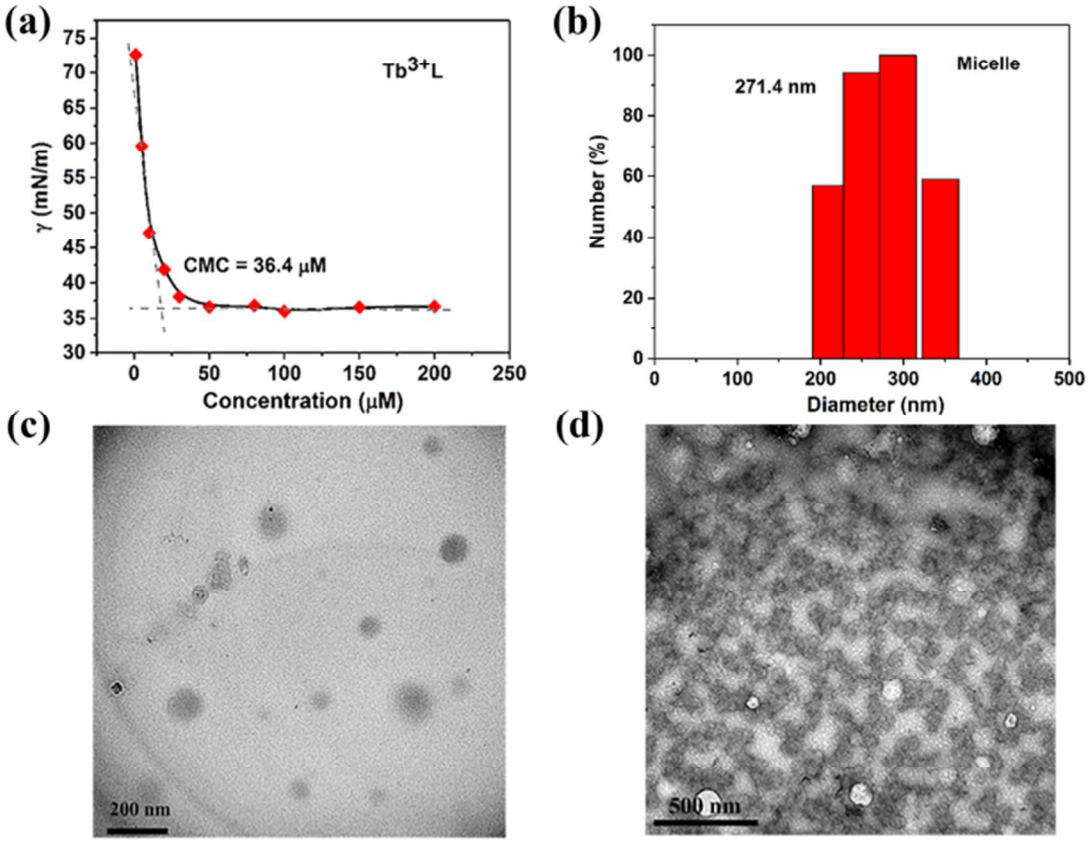

Figure 1. (a) Plot of surface tension as a function of the concentration of the solution of micelle in HEPES buffer (10 mM, pH = 7.0). (b) Particle distribution of terbium functionalized micelle in HEPES buffer (10 mM, pH = 7.0) solution measured by DLS. TEM image of terbium functionalized micelle (c) the grid was untreated and (d) the grid was post-stained with uranyl acetate.

The binding of Tb^{3+} ions to ligand L was also identified by ζ potential (Table S1). The ζ potential of Tb^{3+}-L micelle (ζ = 72.2 mV) showed a significant increase in comparison to the ζ potential of ligand L micelle (ζ = 39.2 mV), which indicated that Tb^{3+} ions incorporated in micelle surfaces. In addition, it can be seen that Tb^{3+}-L micelle formed nanoparticle with an average diameter of 269.5 nm is larger than the nanoparticle formed with ligand L (an average diameter, 193.6 nm) (Figure S1a). Through the above characterization, the coordinated interaction between Tb^{3+} ions and ligand L can be demonstrated. The Tb^{3+} content (29.5 %) in micelle was obtained by thermogravimetric analysis (TGA) (Figure S3). It can be calculated that the complex ratio of ligand L to Tb^{3+} is approximately 1 : 2.

Optical responses of micelle as nanoprobe for DPA detection

The ability of terbium functionalized micelle for ratiometric detection of DPA was then investigated. Firstly, the stability of fluorophore as the fluorescent reference was measured by the detection of the fluorescence of FR at different pH in aqueous solution. The fluorescence of fluorophore exhibited ignorable change within a large pH range (5.0-10.0), which reveals that the pH of solution has a negligible influence on the fluorescence of FR (Figure S4). The results indicated that the micelles have reliable capacity as the ratiometric fluorescence nanoprobe for detecting bio-relevant molecules. Then the photophysical characteristics of Tb^{3+}-L micelles were measured in HEPES buffer (10 mM，pH = 7.0). The micelle only showed blue luminescence (the fluorescence

of FR, 440 nm) in aqueous solution under UV irradiation (275 nm). Interestingly, upon addition of 5 μM DPA, the aqueous of terbium functionalized micelle showed the intrinsic absorption peak of DPA and gave a significant bright green luminescence (Figure S5). In the emission spectrum, the emission bands were observed at 495 nm ($^5D_4 \rightarrow {}^7F_6$), 545 nm ($^5D_4 \rightarrow {}^7F_5$), 586 nm ($^5D_4 \rightarrow {}^7F_4$), and 621 nm ($^5D_4 \rightarrow {}^7F_3$) under 275 nm excitation (Figure S6),[53,54] which were intrinsic bands of Tb^{3+} ions. As neither of the micelle nor DPA alone showed any green luminescence under these conditions, Tb^{3+} ions were sensitized and emitted characteristic luminescence, which was attributed that the coordinated H_2O is replaced by DPA from the lanthanide center and DPA as the "antenna" molecule transferring energy to Tb^{3+} ions. The binding of DPA to the micelles was also confirmed by ζ potential changes. The ζ value of the micelles showed pronounced decrease from 20.17 mV to 0.48 mV after addition of 100 μM DPA (Table S1). Although coordination between DPA and Tb^{3+} ions reduced the surface charge of the micelle, the obtained micelles remained monodisperse (Figure S7) and the particle diameter has no significant change (Figure S8). The terbium functionalized micelle can be used for precise ratiometric fluorescence detection of DPA concentration due to the emission intensity of Tb^{3+} ions increased significantly while the reference emission intensity at 440 nm hardly changed.

The optical sensing property of micelle for DPA was investigated further in HEPES buffer solution (10 mM, pH = 7.0) at room temperature. With addition of DPA, the

terbium functionalized micelle emitted stronger and stronger green fluorescence with negligible change in the fluorescence intensity of FR and the fluorescence enhancement of Tb^{3+} ions in the micelle reached a plateau in seconds. Since the characteristic fluorescence intensity of Tb^{3+} ions at 545 nm was highest increase upon addition of DPA, the fluorescence intensity change at 545 nm was set to quantitatively detect DPA (Figure S6). It was also investigated that the effect of pH on the fluorescence intensity ratio (I_{545} / I_{440}) of the micelles when DPA was added (Figure S9). The I_{545} / I_{440} was found to vary slightly from pH = 5.0 to 9.0, and decreased sharply at higher pH (pH = 10.0) on account of the formation of Tb^{3+} hydroxide and precipitated. The result indicated that the micelle nanoprobe can be used to detect DPA at normal pH range. Then the sensitivity of lanthanide functionalized micelle to detect DPA was investigated through measuring the fluorescence changes when different concentration of DPA was added into the aqueous solution of lanthanide functionalized micelle. As the Figure 2a shows, the fluorescent intensity at 545 nm gradually increases with the DPA concentration of 0 μM to 18 μM, and the fluorescent intensity at 440 nm was almost invariant. The intensity of fluorescence emission at 545 nm was observably enhanced about 140 fold when the concentration of DPA was increased to 18 μM (Figure S10). The fluorescent intensity ratio of the peak at 545 nm and 440 nm showed linear variation with $R^2 = 0.999$ in the range of 0 μM to 7 μM DPA (Figure 2b). Moreover, the detection limit of the lanthanide functionalized micelle for DPA was calculated to be about 54 nM from the calibration curve using the method of signal-to-noise ratio (S / N) of 3, which is lower than the

detection limit (87 nM, R^2 = 0.998) by measuring "turn-on" fluorescence at 545 nm (Figure S10), which is sufficient for the detection of anthrax spore stock suspension.[55] It was obviously demonstrated that ratiometric fluorescence detection own superiority over single-fluorescence detection. The luminescence of the aqueous of lanthanide functionalized micelle changed from blue to green emission upon adding 60 μM DPA (the infectious dose in anthrax spores), which can be distinctly visible under 254 nm UV-lamp illumination (Figure 2a inset).[22] Interestingly, the fluorescence intensity of Tb^{3+} linearly changes with the increase of DPA concentration, so it can be easily changed the detection range by adjusting concentration of micelles. The fluorescence titration curve showed the micelle and DPA concentrations combined with a 1 : 1.25 binding model (Figure S11) and stability constant (K_S) was 2.17×10^{10} L mol^{-1} (Figure S12).[56] The ratiometric sensing capability of the micelle can be used for rapidly and quantitatively analyzing the concentration of DPA without being influenced by external condition arising from instrumental or environmental factors.

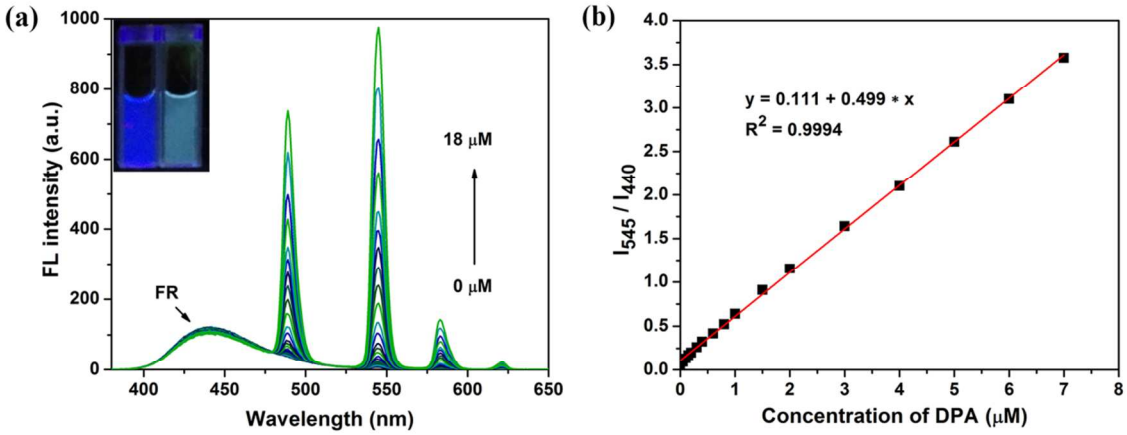

Figure 2. (a) Fluorescent spectra changes of micelle (50 μg·mL^{-1}) upon addition of different concentrations of DPA (0-18 μM) in HEPES buffer (10 mM, pH = 7.0) at room temperature, slit: 5 nm / 3 nm. (Inset: photographs of the fluorescence of micelle before (left) and after (right) adding 60 μM DPA under a UV lamp at 254 nm) (b) Linear relationship of the fluorescence intensity (I_{545} / I_{440}) against the concentration of DPA from 0 to 7 μM. The data were reported as the mean ± standard deviation of triplicate experiments and were fitted by the equation inserted.

High selectivity is very crucial to a probe, thus the selectivity of lanthanide functionalized micelle for DPA was evaluated by addition of various other aromatic ligands or amino acid. As showed in Figure 3, upon addition of benzoic acid (BA), o-phthalic acid (o-PA), m-phthalic acid (m-PA), p-phthalic acid (p-PA), glutamine (Glu), glycine (Gly), methionine (Met) and phenylalanine (Phe), the fluorescence intensity of the lanthanide functionalized micelle (50 mg·mL^{-1}) didn't show noticeable change. Moreover, competition experiments showed that the luminescent response of lanthanide

functionalized micelle to DPA was not interfered by all of these aromatic ligands and amino acid. The high selectivity of lanthanide functionalized micelle for DPA can be attributed that the carboxylate groups and nitrogen atom in the pyridine ring of DPA can provide strong interactions with Tb^{3+} ions. In the opposite, other aromatic ligands may not sufficiently chelate with Tb^{3+} ions. Further, the lowest triplet level of the DPA ($^3\pi\pi^*$) is more suitable for transferring energy from the ligand to the metal ion, so that Tb^{3+} ions can be sensitized and emit intrinsic fluorescence. The coordination interaction between Tb^{3+} and DPA was demonstrated on the basis of the details in the support information. The experiment results indicate that almost two H_2O molecules coordinate with Tb^{3+} ion in the micelle. And the number of H_2O molecules has negligible change upon addition of DPA into the aqueous of terbium functionalized micelle. And we deduce that the DPA may replace the coordinated anion and enter in the coordination sphere of Tb^{3+} through metal-ligand chelate coordination and ion-pairing mutual effect.[57]

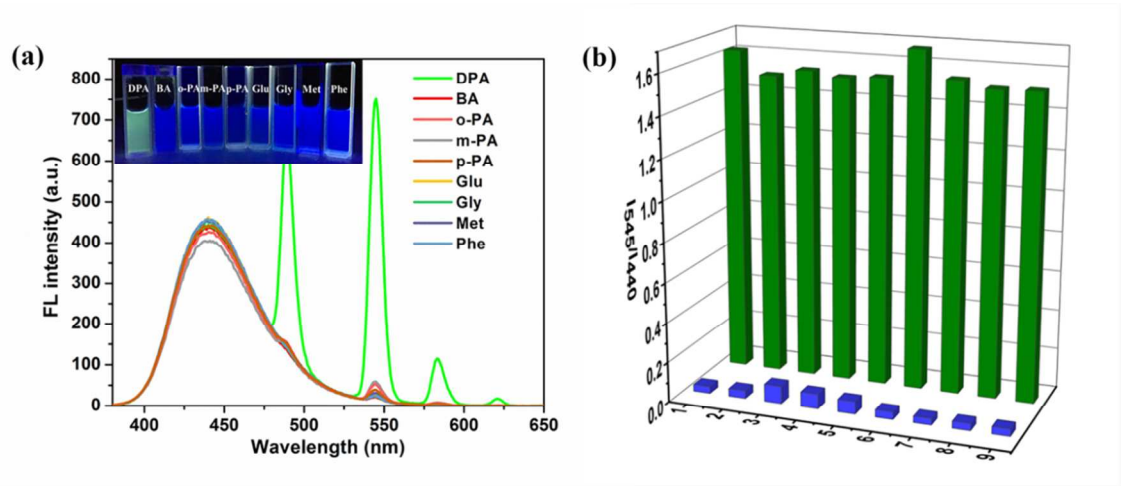

Figure 3. Fluorescence responses of terbium functionalized micelle toward different potentially interfering aromatic ligands or amino acids. (a) Fluorescent spectra of micelle in the presence of 5 μM DPA, BA, o-PA, m-PA, p-PA, Glu, Gly, Met or Phe, slit: 5 nm / 5 nm. (Inset: photographs of the fluorescence of micelle upon addition of different analytes under a UV lamp at 254 nm). (b) The blue bars represent addition of 5 μM analytes to a 50 mg·mL^{-1} solution of micelle (pH = 7.0, HEPES buffer solution): (1) blank, (2) BA, (3) o-PA, (4) m-PA, (5) p-PA, (6) Glu, (7) Gly, (8) Met, (9) Phe. The green bars represent subsequent addition of 5 μM DPA to the mixture. The excitation wavelength was set to 275 nm.

Overall, these results clearly proved that lanthanide functionalized micelle own excellent selectivity and anti-interference ability for effective recognition of anthrax spores biomarker. Furthermore, when DPA was introduced into the aqueous of lanthanide functionalized micelle, the micelle showed a rapid fluorescence response, and the luminescence of Tb^{3+} ions reached a plateau within seconds. As compared to previously

lanthanide(III)-based probe (Table S2), the terbium functionalized micelle was constructed through self-assembly, with excellent biocompatibility and broad detection range. Thus, the lanthanide functionalized micelle nanoprobe was allowed for rapid detection of anthrax spore biomarker.

Application of terbium functionalized micelle

To investigate the application performance of the terbium functionalized micelle nanoprobe, the silica gel plate was impregnated with the micelle nanoprobe as test paper for detection of DPA. As shown in Figure 4a, the silica gel plate impregnated with DPA solution (60 μM, 0.5 mL) emitted green fluorescence under the irradiation of a UV lamp (254 nm). In the opposite, the silica gel plate impregnated with other analyte solution (60 μM, 0.5 mL) only emitted the blue fluorescence of FR. Then, we used the solution of DPA as ink, and the pre-processed silica gel sheet as paper. After writing by DPA, the portion of silica gel plate written by DPA showed green fluorescence under a UV lamp at 254 nm (Figure 4b), and the plate had no color change under visible light. Therefore, the device pretreated with terbium functionalized micelle has potential capacity as test paper for detecting anthrax spore biomarker, and may have application in the security.

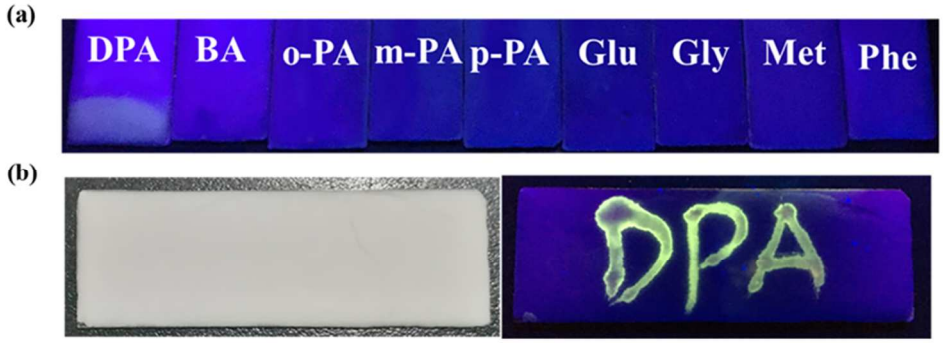

Figure 4. (a) The photographs of the fluorescence of silica gel plate impregnated with different analytes (60 μM, 0.5 mL) under a UV lamp at 254 nm. (b) The color changes of silica gel plate under visible light (left) and under UV lamp at 254 nm (right) after writing by DPA solution (1 $mM \cdot L^{-1}$).

CONCLUSIONS

In summary, we have successfully developed a lanthanide functionalized micelle nanoprobe for ratiometric fluorescence detection of the anthrax spore biomarker, DPA. The lanthanide functionalized micelle exhibited excellent selectivity and sensitivity to DPA (detection limit 54 nM), which can be attributed to the emitted fluorescence of Tb^{3+} ions sensitized by DPA. When different concentration of DPA was added into the aqueous of lanthanide functionalized micelle, the luminescence of Tb^{3+} ion in the micelle enhanced linearly and the fluorescence of FR remained constant. Therefore, a lanthanide functionalized micelle nanoprobe for ratiometric fluorescence detection of DPA was constructed, which can response to DPA within seconds, and the detection range can be easily changed by adjusting the concentration of the micelle. The lanthanide

functionalized self-assembled micelle would provide a new strategy for designing ratiometric fluorescence nanoprobe to sensitively and rapidly detect bacterial spore biomarker, biomolecules or other applications.

ASSOCIATED CONTENTS

Supporting Information

Synthesis of FR and Tb^{3+}-L micelle, DLS and TEM measurement, spectrometric properties of micelle, calculating stability constant, luminescence decay curves, ^{1}H NMR, ^{13}C NMR, MS. This material is available free of charge via the Internet at http://pubs.acs.org.

AUTHOR INFORMATION

Corresponding Author

*Email: tangyu@lzu.edu.cn. Fax: +86 931-891-2582. Tel: +86 931-891-2552.

Notes

The authors declare no competing financial interest.

ACKNOWLEDGEMENT

This study has been financially supported by the National Natural Science Foundation of China (Projects 21471071, 21431002) and Fundamental Research Funds for the Central Universities Grants (Project lzujbky-2017-Ot05).

REFERENCES

(1) Goel, A. K. *World J. Clin. Cases* **2015**, *3*, 20-33.
(2) Bhardwaj, N.; Bhardwaj, S.; Mehta, J.; Kim, K. H.; Deep, A. *Biosens. Bioelectron.* **2016**, *86*, 799-804.
(3) King, D.; Luna, V.; Cannons, A.; Cattani, J.; Amuso, P. *J. Clin. Microbiol.* **2003**, *41*, 3454-3455.
(4) Zhang, B. H.; Wang, H. S.; Lu, L. H.; Ai, K. L.; Zhang, G.; Cheng, X. L. *Adv. Funct. Mater.* **2008**, *18*, 2348-2355.
(5) Huan, T. N.; Ganesh, T.; Han, S. H.; Yoon, M. Y.; Chung, H. *Biosens. Bioelectron.* **2011**, *26*, 4227-4230.
(6) Enserink, M. *Science* **2001**, *294*, 490-491.
(7) Zhang, X. Y.; Zhao, J.; Whitney, A. V.; Elam, J. W.; Van Duyne, R. P. *J. Am. Chem. Soc.* **2006**, *128*, 10304-10309.
(8) Paulus, H. *Anal. Biochem.* **1981**, *114*, 407-410.
(9) Tan, C. L.; Wang, Q. M.; Zhang, C. C. *Chem. Commun.* **2011**, *47*, 12521-12523.
(10) Hurtle, W.; Bode, E.; Kulesh, D. A.; Kaplan, R. S.; Garrison, J.; Bridge, D.; House, M.; Frye, M. S.; Loveless, B.; Norwood, D. *J. Clin. Microbiol.* **2004**, *42*, 179-185.
(11) Zhang, X. Y.; Young, M. A.; Lyandres, O.; Van Duyne, R. P. *J. Am. Chem. Soc.* **2005**, *127*, 4484-4489.
(12) Li, Q.; Sun, K.; Chang, K. W.; Yu, J. B.; Chiu, D. T.; Wu, C. F.; Qin, W. P. *Anal. Chem.* **2013**, *85*, 9087-9091.
(13) Hang, J.; Sundaram, A. K.; Zhu, P. X.; Shelton, D. R.; Karns, J. S.; Martin, P. A. W.; Li, S. H.; Amstutz, P.; Tang, C. M. *J. Microbiol. Meth.* **2008**, *73*, 242-246.
(14) Goodacre, R.; Shann, B.; Gilbert, R. J.; Timmins, E. M.; McGovern, A. C.; Alsberg, B. K.; Kell, D. B.; Logan, N. A. *Anal. Chem.* **2000**, *72*, 119-127.
(15) Ai, K. L.; Zhang, B. H.; Lu, L. H. *Angew. Chem., Int. Ed.* **2009**, *48*, 304-308.
(16) Tsukube, H.; Shinoda, S. *Chem. Rev.* **2002**, *102*, 2389-2403.
(17) Kupcho, K. R.; Stafslien, D. K.; DeRosier, T.; Hallis, T. M.; Ozers, M. S.; Vogel, K. W. *J. Am. Chem. Soc.* **2007**, *129*, 13372-+.
(18) Hanaoka, K.; Kikuchi, K.; Kobayashi, S.; Nagano, T. *J. Am. Chem. Soc.* **2007**, *129*, 13502-13509.
(19) Hindle, A. A.; Hall, E. A. H. *Analyst* **1999**, *124*, 1599-1604.
(20) Curiel, D.; Sanchez, G.; Mas-Montoya, M.; Tarraga, A.; Molina, P. *Analyst* **2012**, *137*, 5499-5501.
(21) Binnemans, K. *Chem. Rev.* **2009**, *109*, 4283-4374.(22) Chen, H.; Xie, Y.; Kirillov, A. M.; Liu, L.; Yu, M.; Liu, W.; Tang, Y. *Chem. Commun.* **2015**, *51*, 5036-5039.
(23) Sun, Y. P.; Zhou, B.; Lin, Y.; Wang, W.; Fernando, K. A. S.; Pathak, P.; Meziani, M. J.; Harruff, B. A.; Wang, X.; Wang, H. F.; Luo, P. J. G.; Yang, H.; Kose, M. E.; Chen, B. L.; Veca, L. M.; Xie, S. Y. *J. Am. Chem. Soc.* **2006**, *128*, 7756-7757.
(24) Feng, L.; Liu, Y. W.; Tang, X. Y.; Piao, Y. M.; Chen, S. F.; Deng, S. L.; Xie, S. Y.; Wang, Y. H.; Zheng, L. S. *Chem. Mater.* **2013**, *25*, 4487-4496.
(25) Zhang, Y.; Li, B.; Ma, H.; Zhang, L.; Zheng, Y. *Biosens. Bioelectron.* **2016**, *85*, 287-293.
(26) Yilmaz, M. D.; Hsu, S. H.; Reinhoudt, D. N.; Velders, A. H.; Huskens, J. *Angew. Chem., Int. Ed.* **2010**, *49*, 5938-5941.
(27) Oh, W. K.; Jeong, Y. S.; Song, J.; Jang, J. *Biosens. Bioelectron.* **2011**, *29*, 172-177.

(28) Xu, H.; Rao, X.; Gao, J.; Yu, J.; Wang, Z.; Dou, Z.; Cui, Y.; Yang, Y.; Chen, B.; Qian, G. *Chem. Commun.* **2012**, *48*, 7377-7379.
(29) Tan, H.; Ma, C.; Chen, L.; Xu, F.; Chen, S.; Wang, L. *Sens. Actuators B* **2014**, *190*, 621-626.
(30) Wang, Y.; Li, Y.; Qi, W.; Song, Y. *Chem. Commun.* **2015**, *51*, 11022-11025.
(31) Ma, B. L.; Zeng, F.; Zheng, F. Y.; Wu, S. Z. *Analyst* **2011**, *136*, 3649-3655.
(32) Chen, Y.; Zhu, C.; Yang, Z.; Chen, J.; He, Y.; Jiao, Y.; He, W.; Qiu, L.; Cen, J.; Guo, Z. *Angew. Chem., Int. Ed.* **2013**, *52*, 1688-1691.
(33) Forzani, E. S.; Lu, D. L.; Leright, M. J.; Aguilar, A. D.; Tsow, F.; Iglesias, R. A.; Zhang, Q.; Lu, J.; Li, J. H.; Tao, N. J. *J. Am. Chem. Soc.* **2009**, *131*, 1390-1391.
(34) Ma, X.; Zhao, Y. L. *Chem. Rev.* **2015**, *115*, 7794-7839.
(35) Peng, H. Q.; Niu, L. Y.; Chen, Y. Z.; Wu, L. Z.; Tung, C. H.; Yang, Q. Z. *Chem. Rev.* **2015**, *115*, 7502-7542.
(36) Ramanathan, M.; Shrestha, L. K.; Mori, T.; Ji, Q. M.; Hill, J. P.; Ariga, K. *Phys. Chem. Chem. Phys.* **2013**, *15*, 10580-10611.
(37) Zheng, L. Z.; Li, J. H. *J. Phys. Chem. B* **2005**, *109*, 1108-1112.
(38) Zhu, J. H.; Yu, C.; Chen, Y.; Shin, J.; Cao, Q. Y.; Kim, J. S. *Chem. Commun.* **2017**, *53*, 4342-4345.
(39) Zhou, Z.; Song, J.; Tian, R.; Yang, Z.; Yu, G.; Lin, L.; Zhang, G.; Fan, W.; Zhang, F.; Niu, G.; Nie, L.; Chen, X. *Angew. Chem., Int. Ed.* **2017**, *56*, 6492-6496.
(40) Liu, J.; Morikawa, M. A.; Lei, H.; Ishiba, K.; Kimizuka, N. *Langmuir* **2016**, 32, 10597-10603.
(41) Polarz, S.; Landsmann, S.; Klaiber, A. *Angew. Chem., Int. Ed.* **2014**, *53*, 946-954.
(42) Lanigan, N.; Wang, X. *Chem. Commun.* **2013**, *49*, 8133-8144.
(43) Lei, H.; Liu, J.; Yan, J.; Lu, S.; Fang, Y. *ACS Appl. Mater. Interfaces* **2014**, *6*, 13642-13647.
(44) Liu, J.; Morikawa, M.-a.; Kimizuka, N. *J. Am. Chem. Soc.* **2011**, *133*, 17370-17374.
(45) Lei, H.; Liu, J.; Yan, J.; Quan, J.; Fang, Y. *Langmuir* **2016**, *32*, 10350-10357.
(46) Wei, X.; Dong, R.; Wang, D.; Zhao, T.; Gao, Y.; Duffy, P.; Zhu, X.; Wang, W. *Chem. - Eur. J.* **2015**, *21*, 11427-11434.
(47) Yao, Y.; Xue, M.; Chen, J.; Zhang, M.; Huang, F. *J. Am. Chem. Soc.* **2012**, *134*, 15712-15715.
(48) Shau, S. M.; Chang, C. C.; Lo, C. H.; Chen, Y. C.; Juang, T. Y.; Dai, S. A.; Lee, R. H.; Jeng, R. J. *ACS Appl. Mater. Interfaces* **2012**, *4*, 1897-1908.
(49) Luo, X.; Chen, M.; Zhang, Y.; Chen, Z.; Li, X. *Chem. - Eur. J.* **2016**, *98*, 9-19.
(50) Cao, Y.; Liu, M.; Zhang, K.; Zu, G.; Kuang, Y.; Tong, X.; Xiong, D.; Pei, R. *Biomacromolecules* **2017**, *18*, 150-158.
(51) Abbas, Z.; Dasari, S.; Patra, A. K. *RSC Adv.* **2017**, *7*, 44272-44281.
(52) Lincheneau, C.; Leonard, J. P.; McCabe, T.; Gunnlaugsson, T. *Chem. Commun.* **2011**, *47*, 7119-7121.
(53) Li, G.; Zhang, Y.; Geng, D.; Shang, M.; Peng, C.; Cheng, Z.; Lin, J. *ACS Appl. Mater. Interfaces* **2012**, *4*, 296-305.
(54) de Faria, E. H.; Nassar, E. J.; Ciuffi, K. J.; Vicente, M. A.; Trujillano, R.; Rives, V.; Calefi, P. S. *ACS ACS Appl. Mater. Interfaces* **2011**, *3*, 1311-1318.
(55) Cable, M. L.; Kirby, J. P.; Levine, D. J.; Manary, M. J.; Gray, H. B.; Ponce, A. *J. Am. Chem. Soc.* **2009**, *131*, 9562-9570.
(56) Liu, G.; Feng, D.-Q.; Mu, X.; Zheng, W.; Chen, T.; Qi, L.; Li, D. *J. Mater. Chem. B* **2013**, *1*, 2128.

(57) Salvia, M. V.; Ramadori, F.; Springhetti, S.; Diez-Castellnou, M.; Perrone, B.; Rastrelli, F.; Mancin, F. *J. Am. Chem. Soc.* **2015**, *137*, 886-892.

FOR TOC ONLY：

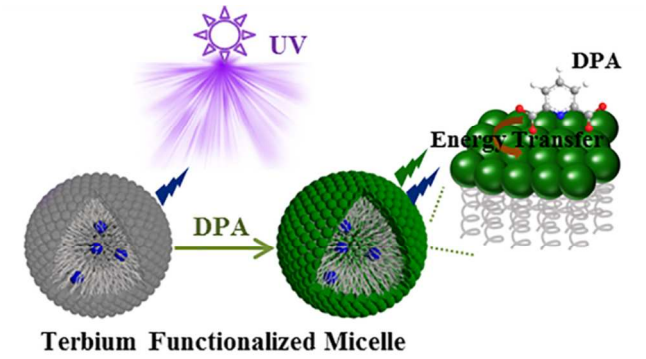
UV
DPA
Energy Transfer
DPA
Terbium Functionalized Micelle